THE USE OF INVERSE SIMULATION FOR CONCEPTUAL DESIGN

D.G. Thomson
and
R. Bradley

Department of Aerospace Engineering
University of Glasgow
Glasgow
G12 8QQ
Scotland

Abstract

The calculation of the control inputs required to fly a predefined manoeuvre is known as inverse simulation. When the mathematical model used is generic, inverse simulation can be used to measure the effect on the performance of the helicopter due to parametric changes. The choice of which manoeuvres are to be simulated is made easier by referring to the U.S. Aeronautical Design Standards for the handling qualities of military rotorcraft which defines a series of Mission Task Elements to be flown within specified performance limits. Mathematical representations of some of these manoeuvres are developed in this paper, and the use of inverse simulation for design purposes is demonstrated by a series of simulations of a hypothetical helicopter configuration flying them.

Nomenclature

g	Acceleration due to gravity
h	Lateral displacement in slalom
k	Fraction of turn manoeuvre in entry and exit transients
n	Load factor
R	Radius of circular track
t	Time
t_m	Manoeuvre time
V	Flight velocity
x, y, z	Helicopter position relative to earth fixed origin
β	Fuselage sideslip angle
χ	Track angle
$\dot{\chi}$	Turn rate
γ	Angle of climb
θ	Fuselage pitch angle
θ_0	Main rotor collective pitch angle
θ_{0tr}	Tail rotor collective pitch angle
θ_{1s}	Main rotor longitudinal cyclic pitch angle
θ_{1c}	Main rotor lateral cyclic pitch angle
ϕ	Fuselage roll angle
ψ	Fuselage heading angle

1. Introduction

A consequence of improved mathematical modelling techniques is that confidence in the use of simulations during the design process is increased. In particular, at the very earliest stage of design where new concepts or configurations are under investigation, the use of a simulation incorporating a generic mathematical model will allow the effect of changes in key configurational parameters to estimated. The importance of simulation in new designs is acknowledged by the authors of the U.S. Military Rotorcraft Handling Qualities Requirements ADS-33C [1] who state that 'compliance with the requirements will be demonstrated using analysis, simulation and flight test at appropriate milestones during the rotorcraft design and development'. The work described in this paper demonstrates how inverse simulation is particularly valuable as a general purpose design tool and how it can be used to help demonstrate and achieve compliance with handling qualities requirements.

Inverse simulation takes a predefined flight path, or trajectory and calculates the control inputs necessary to fly it, and has found an application in control system design and analysis for fixed wing aircraft [2,3]. Recently Nannoni and Stabellini [4] used a simplified inverse simulation to assess control inputs and power requirements for take-off and landing. At the University of Glasgow, inverse simulation for rotorcraft has received considerable attention, [5,6,7] mainly in relation to flight mechanics applications. The simulation is implemented in a package 'HELINV', discussed in section 2 below, which incorporates a nonlinear, generic, helicopter mathematical model. The generic nature of the model enables a wide variety of configurations and design options to be explored.

The particular area of the requirements that has received attention here is that devoted to aggressive tasks. A prerequisite for the defined tasks, or Mission Task Elements (MTEs) as they are known, to be a subject of inverse simulation, is that they have to be translated into precise flight paths. The manner in which this is to be done is not always unambiguous, and there is scope for a variety of interpretations. The conversions from MTEs to flight paths are discussed in some detail in section 3 of this paper.

It should be emphasised that the focus of interest is on conceptual design, even though inverse simulation is being applied to the MTEs of the Handing Qualities Requirements. The Aeronautical Design Standard for rotorcraft handling qualities, ADS-33C [1] identifies the following four steps as a progression of evaluation during design development and demonstration of compliance:

(i) analytical checks computed using available math models
(ii) analytical checks using full nonlinear math models
(iii) pilot assessments using flight simulators
(iv) flight test verification

Inverse simulation has a part to play in this sequence of development. It can establish, for a particular rotorcraft configuration, the inherent capability of flying a manoeuvre in the required manner, and so answer the question "given an ideal pilot, how will the rotorcraft behave when flying this manoeuvre, and what control actions will be required of him ?"

The control-input time history must influence the workload experienced by the pilot and the attitude taken up by the rotorcraft at critical stages of the manoeuvre may effect his cue environment. It follows that the results from inverse simulation must impact in some way on handling qualities, but, as yet, there is no direct path from inverse simulation to handling qualities quantification. As a consequence, the discussion in this paper is confined to the use of inverse simulation and MTEs in conceptual design and evaluation of alternative configurations. Some examples of inverse simulation studies are provided in section 4.

Before describing how inverse simulation can be used as a design tool, a brief summary of the package and its applications is perhaps appropriate (a comprehensive description of the inverse simulation package HELINV, is given by Thomson and Bradley [5]).

2. The Helicopter Inverse Simulation Package HELINV

The initial intention of creating an inverse simulation was to investigate, and ultimately to evaluate, helicopter agility [8]. From this work it was clear that there were other potential uses for inverse simulation, particularly in the investigation of constrained flight [7], pilot control strategy [6], and as a model validation tool [9,10]. Three main elements of the simulation are presented here, followed by a discussion of the validity of the technique.

2.1 The Mathematical Model

In developing HELINV use has been made of the Royal Aerospace Establishment's helicopter mathematical model, HELISTAB. This is a generic model of a single main and tail rotor helicopter where the helicopter configuration is defined by a series of key parameters. The version used is a seven degrees of freedom (six body degrees plus the rotor speed) nonlinear model, although higher order models with flapping degrees of freedom are available. The rotor blades are assumed to be rigid, have constant chord and lift curve slope, and the flow around them is assumed to be steady and incompressible. Blade flapping behaviour is simulated by use of a centre spring representation, coupling between blade pitch and lag motions is ignored, and the rotor forces and moments are calculated by assuming quasi-steady flapping and coning. Fuselage, tailplane and fin forces and moments are found from empirical formulae which were developed from wind tunnel data. Complete details of the model are given by Padfield [11].

2.2 Defining Helicopter Manoeuvres

An inverse simulation of any dynamic system must begin by defining the required system output. When the system being simulated is a helicopter, this output consists of a manoeuvre. A series of nap-of-the-earth manoeuvres, such as bob-up, side-step, and turns have been modelled for use with HELINV (detailed descriptions are given by Thomson and Bradley [12]). A manoeuvre is assumed to be composed of both the flight path (x, y, z), taken to be the position of the helicopter's centre of gravity relative to an earth fixed axes system, and information on the direction in which the fuselage is pointing. This is given by the heading angle, ψ (the angle between earth and body fixed x axes), which is either explicitly defined as a function of time, or in the case of turning flight, is found from a predefined sideslip angle function $\beta(t)$ [5]. Simple mathematical functions which give appropriate flight path geometries are used to specify these parameters. The requirement to define aircraft heading originates from the desire to produce a unique solution, i.e. the calculation of a single set of control inputs which, if applied to the helicopter, will result in the defined manoeuvre being flown. As the helicopter has four controls, four constraints must be applied to its motion to achieve this. In general terms, main rotor collective is used to control displacements in the z-direction, with longitudinal and lateral cyclic controlling displacements in the x and y directions respectively. This leaves tail rotor collective as the remaining control, and it follows that heading angle will be a suitable fourth constraint.

2.3 The Inverse Simulation Algorithm

One of the most fundamental prerequisites of a helicopter inverse simulation is the ability to calculate the fuselage rotational and translational velocities and accelerations required to fly specified manoeuvre. In HELINV, the velocities and accelerations are given in earth axes by the manoeuvre definitions and therefore must be transformed by rotations through the Euler angles, roll, ϕ, pitch, θ, and heading, ψ, into body axes. The heading angle is predefined, as discussed above, and the roll and pitch angles are taken to be the unknown variables in a Newton-Raphson iterative scheme used to solve the equations of motion. Body rotational rates and accelerations are calculated using numerical differentiation of the Euler angles. Knowledge of the body translational velocities, the rotational rates, and the attitude angles permits the aerodynamic and inertial forces and moments of the fuselage, and the forces and moments from the rotor to be calculated. With the inertial, gravitational and external forces and moments now known it is possible to solve the motion equations for the unknown attitude angles. On convergence the control angles are calculated by consideration of the rotor loads and flapping dynamics. The HELINV inverse simulation algorithm is summarised in the flow chart given in Figure 1. The algorithm was verified by generating control inputs for a particular manoeuvre, then using these controls to drive a conventional time response simulation, again using the HELISTAB model.

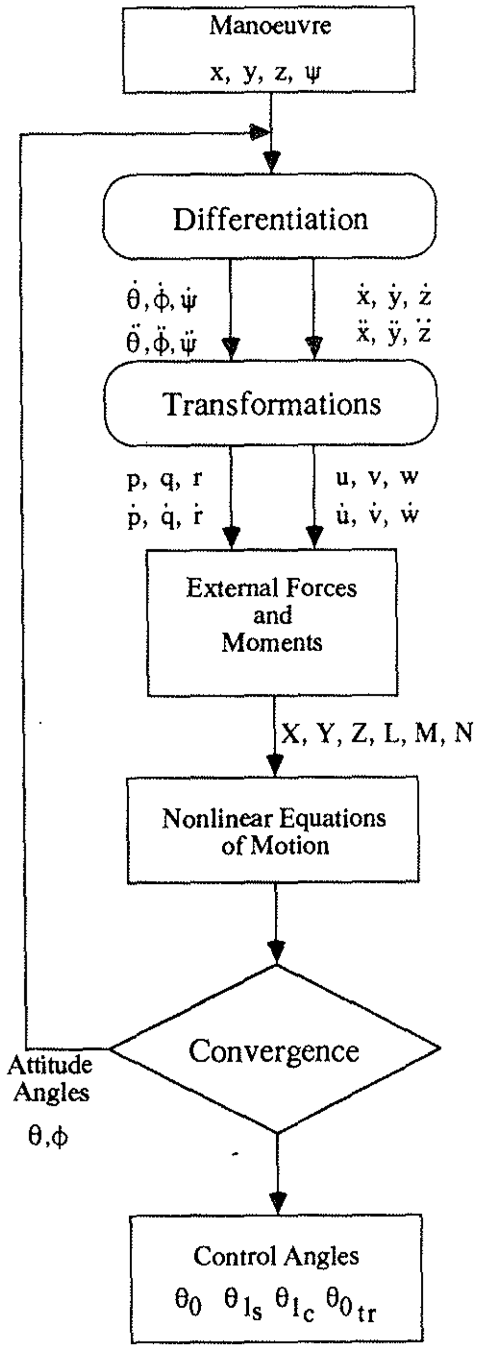

Figure 1 : Block Diagram of the HELINV Inverse Simulation Algorithm

Comparison of the commanded manoeuvre with that generated by the calculated controls is sufficient to verify the algorithm.

2.4 Validity of HELINV Results

An alternative to mathematically defined manoeuvres is to use flight path and heading information from flight tests. Assuming that the control time histories are also recorded during the flight test, there is then a basis for validating the mathematical model by comparing the recorded control time histories with those computed using inverse simulation. This has been investigated recently [9, 10], and the simulation results have shown good correlation with the flight data. This is evident on examination of Figure 2 which shows a comparison of flight test results with an inverse simulation of the identical manoeuvre. In this case the manoeuvre was a 600ft (183m) quick-hop (longitudinal acceleration and deceleration, from hover to hover, over a specified distance), flown by a Westlands Lynx helicopter. Reasonably good correlation is achieved particularly in the plots of collective and fuselage pitch angles. One of the features of the aggressive manoeuvres inherent in many MTEs is that the helicopter is driven to regions of the flight envelope where the authenticity of the mathematical modelling is uncertain. There is a need for flight tests to be conducted over a range of representative manoeuvres to provide data for validation. The limited data that has been available so far has given encouraging comparisons with the results of inverse simulations.

3. Mathematical Representation of Mission Task Elements

As part of the U.S. Military Rotorcraft Handling Qualities Requirements [1] a series of Mission Task Elements (MTEs) have been defined. In order for a new rotorcraft to comply with the regulations the contractor must demonstrate that it can achieve Level 1 handling qualities whilst flying a subset of the MTEs chosen to represent tasks likely to be flown in its operational role. The intention of the current study is to create mathematical representations of some the MTEs for use with inverse simulation. Considering the number, and wide range of MTEs presented in Ref. 1, it is important to establish exactly where inverse simulation will prove to be of most value. The MTEs can be split into 4 groups : Precision Tasks, Aggressive Tasks, Precision Tasks in Degraded Visual Environment, and Moderately Aggressive Tasks in Degraded Visual Environment. The precision tasks include mainly low speed and hover manoeuvres, whilst the aggressive tasks involve manoeuvres where much larger vehicle displacements arise. In both cases the tasks in Degraded Visual Environment are similar to those in normal conditions but with less severe requirements. In choosing the MTEs to be modelled it is important to consider the motive behind using inverse simulation for design purposes - to ensure that the rotorcraft has the required performance to fly the specified MTEs, and, if it has,

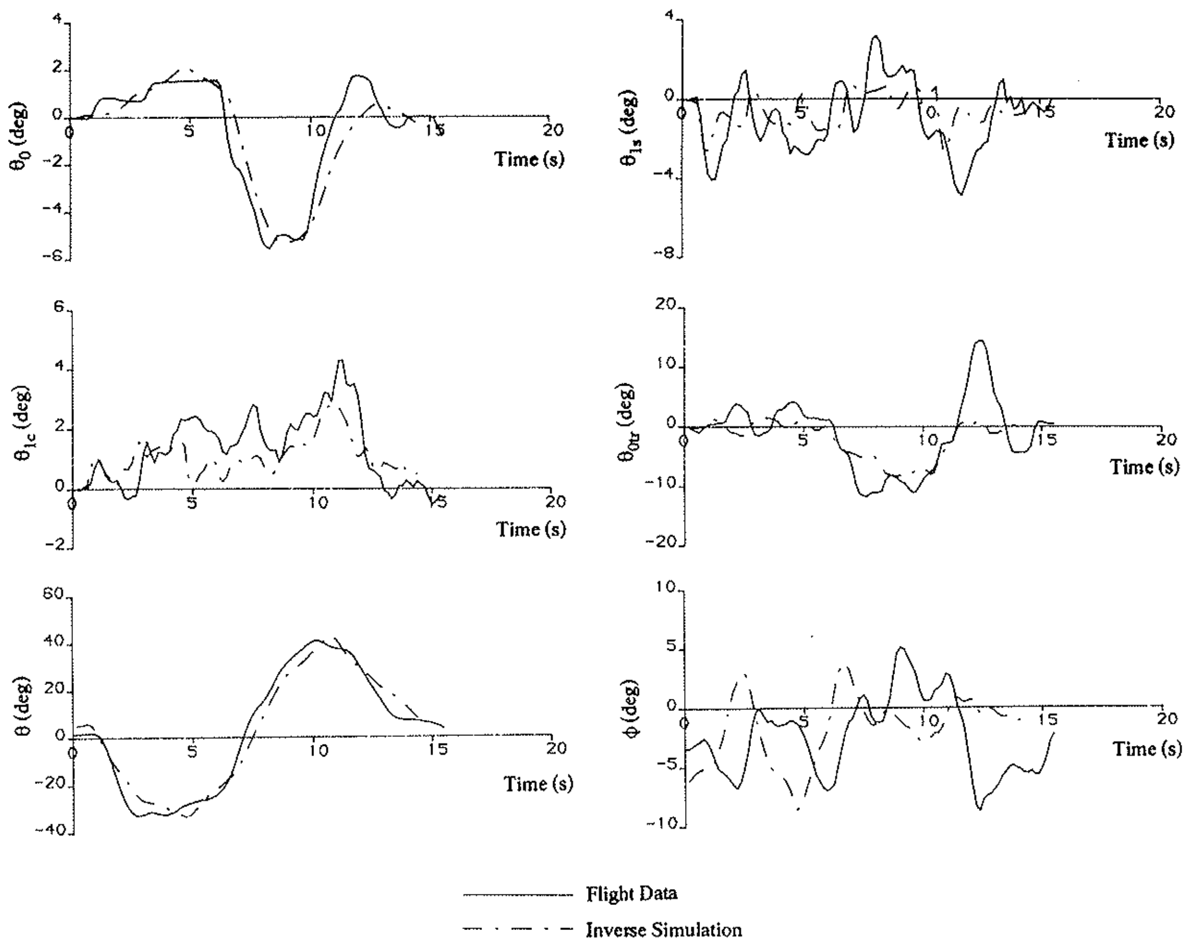

Figure 2 : Comparison of Control and Attitude Time Histories for Westland Lynx Helicopter Flying a 600ft Quick-hop Manoeuvre

how much control margin is available to the pilot . It follows then that inverse simulation will be best suited to modelling the aggressive tasks where control and power limits are much more likely to be approached. Inverse simulation of precision tasks is unlikely to produce much useful information.

The flight path, velocity, acceleration and load factor profiles used to model the MTEs were generated by consideration of the descriptions given in Reference 1. The approach used to model the MTEs is broadly similar to that presented by the authors of Reference 12 where it was shown that there are two possible ways to define a manoeuvre. The most direct way, as mentioned above, is simply to specify the helicopter's position and heading as functions of time. This is not always convenient, and the alternative approach is to specify altitude, turn rate, and velocity so that the manoeuvre specification is given by

$$\dot{\chi} = f_1(t) \tag{1}$$

$$z = f_2(t) \tag{2}$$

$$V = f_3(t) \tag{3}$$

Defining the track angle, χ, and the climb angle, γ, as shown in Figure 3, the component velocities are found to be

$$\dot{x} = V \cos\gamma \cos\chi \tag{4}$$

$$\dot{y} = V \cos\gamma \sin\chi \tag{5}$$

$$\dot{z} = -V \sin\gamma \tag{6}$$

and, as the z component velocity may be found by differentiation of equation (2), and V is specified, equation (3), the climb angle, γ can be found from equation (6). Also, as track angle, χ, may be found by integration of (1), the other component velocities can be found from (4) and (5). Differentiation of equations (2), (4), and (5) will give the earth axes component accelerations. Having determined the flight path, the manoeuvre definition is completed by specifying and appropriate function for heading, ψ, or sideslip angle, β. Descriptions of some of the MTEs now follows.

3.1 Rapid Slalom

The description of this manoeuvre given in Reference 1 states that the manoeuvre is to be initiated in level flight at a constant speed of 60 knots or above. The aircraft is to be displaced laterally to a distance of 15.2m from a centreline marked on the ground, then rolled in the opposite direction to the same distance on the opposite side of the centreline. The manoeuvre is

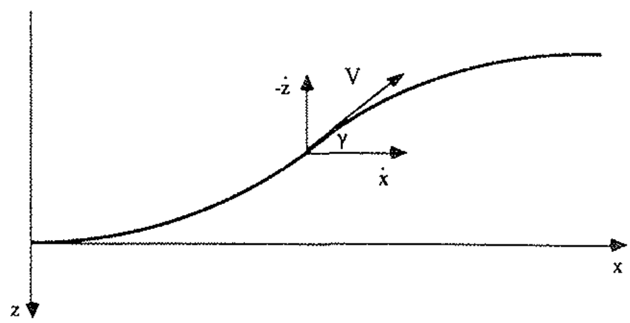

a) Altitude Change in the x-z Plane

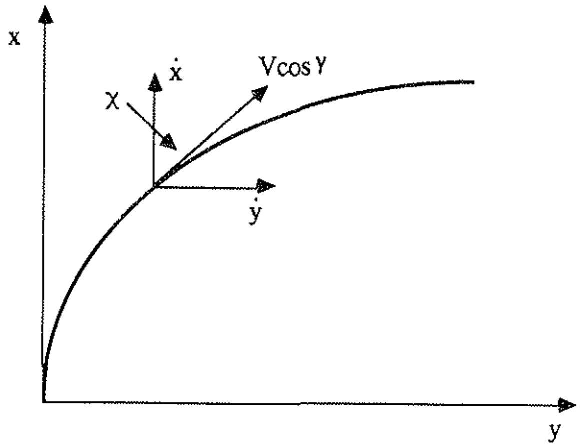

b) Track in the x-y Plane

Figure 3 : Components of a General Manoeuvre

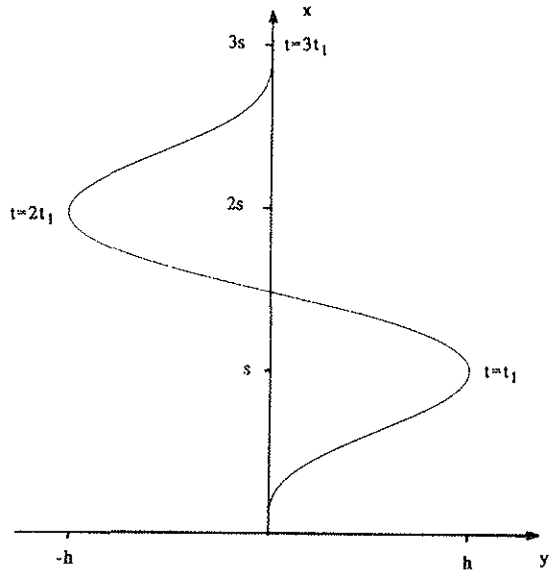

Figure 4 : Track for the Slalom MTE

completed by returning to the centreline. It is also stipulated that the maximum bank angle should be greater than 50 degrees, and the altitude should be maintained below 15.2m. Before a mathematical description of the manoeuvre can be found it is necessary to determine the shape of the flight path. In this case, as it will be assumed that altitude is kept constant, the manoeuvre is simply a track in the earth x-y plane. There are perhaps several possible shapes, the most likely of which is shown in Figure 4, where it is assumed that the manoeuvre is symmetrical. Noting that the flight velocity through the manoeuvre is constant, the lateral displacement, y, can be expressed as a function of time by considering the following boundary conditions

$$\text{i) } t = 0, \quad y = 0, \quad \dot{y} = 0, \quad \ddot{y} = 0$$
$$\text{ii) } t = t_1, \quad y = h, \quad \dot{y} = 0$$
$$\text{iii) } t = 2t_1, \quad y = -h, \quad \dot{y} = 0$$
$$\text{iv) } t = 3t_1, \quad y = 0, \quad \dot{y} = 0, \quad \ddot{y} = 0$$

where h is the lateral displacement of 15.2m. There may be several mathematical functions which could fulfil these conditions, however the simplest is an 8th order polynomial (its nine coefficients being selected to satisfy the nine boundary conditions). This polynomial is found to be of the form

$$y(t) = \left[-2\left(\frac{t}{t_1}\right)^9 + 27\left(\frac{t}{t_1}\right)^8 - 144\left(\frac{t}{t_1}\right)^7 + 378\left(\frac{t}{t_1}\right)^6 - 486\left(\frac{t}{t_1}\right)^5 + 243\left(\frac{t}{t_1}\right)^4\right]\frac{h}{16} \qquad (7)$$

This expression can be differentiated to give the velocity and acceleration in the y-axis direction, and, as altitude is to be kept constant (i.e. z(t)=const.)

$$\dot{z}(t) = 0$$

thus, the velocity in the x-axis direction is given by

$$\dot{x}(t) = \sqrt{V^2 - \dot{y}^2} \qquad (8)$$

The position of the aircraft along the x-axis, and the x-axis component of acceleration can be found by integration and differentiation of equation (8) respectively. To complete the definition of the manoeuvre it is assumed that it is flown without sideslip so that

$$\beta(t) = 0$$

3.2 Acceleration and Deceleration

In this manoeuvre the helicopter is accelerated from the hover to a speed of at least 60 knots, then decelerated back to the hover again. The maximum acceleration is to be achieved within 1.5 seconds from the initiation of the manoeuvre, whilst the maximum deceleration is to occur within 3 seconds of the beginning of the deceleration phase. The whole manoeuvre is to be performed within specified altitude and heading limitations. As the manoeuvre has been described in terms of accelerations, it is convenient to create its mathematical representation in the same way. Taking into account the description above, a suitable acceleration

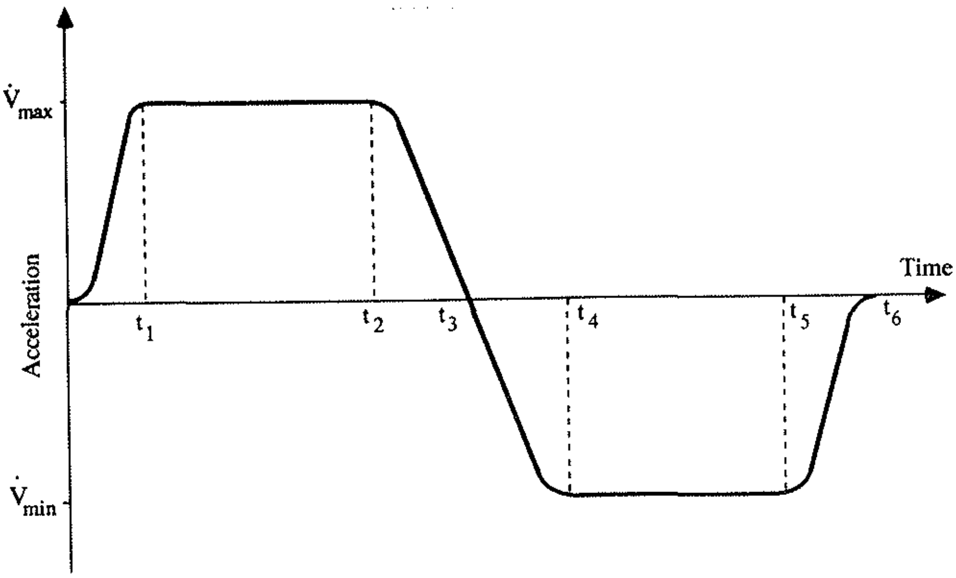

Figure 5 : Acceleration Profile for an Acceleration and Deceleration MTE

profile is given in Figure 5 provided that the following conditions are met

$$t_1 \le 1.5\text{s}, \qquad t_4 - t_3 \le 3\text{s}$$

$$\int_0^{t_3} \dot{V}\, dt \ge 60 \text{ knots} \qquad \int_0^{t_6} \dot{V}\, dt = 0 \tag{9}$$

The above conditions will ensure that the maximum acceleration and deceleration are achieved in the correct times, and also that the specified velocity boundary conditions are met. The main assumption made is that once the maximum acceleration (or deceleration) has been reached, it can be maintained at a constant value until the desired velocity is approached. Two further assumptions about the component times are made:

$$t_6 - t_5 = t_1, \qquad t_4 - t_3 = t_3 - t_2 \tag{10}$$

These assumptions make the manoeuvre symmetrical. Use is made of cubic polynomial transients to initiate and end the manoeuvre, and also to join the constant acceleration and deceleration portions. This gives continuity in higher order derivatives which is desirable in inverse simulation [7]. The coefficients of the cubic polynomial can be found by applying the appropriate boundary conditions. For example, the initial acceleration can be specified by a cubic polynomial of the form

$$\dot{V}(t) = at^3 + bt^2 + ct + d \tag{11}$$

which should have the boundary conditions

$$\text{i) } t = 0,\ \dot{V} = 0, \qquad \ddot{V} = 0$$
$$\text{ii) } t = t_1,\ \dot{V} = \dot{V}_{max},\ \ddot{V} = 0$$

and hence the coefficients for equation (11) are

$$a = \frac{-2\dot{V}_{max}}{t_1^3}, \quad b = \frac{3\dot{V}_{max}}{t_1^2}, \quad c = d = 0$$

The coefficients of the other cubics are found in a similar manner, whilst the component times may be found by integrating the acceleration profile to give the corresponding velocity profile. As the coefficients of the cubic are functions of the component times, the coefficients and times are calculated simultaneously, the component times t_2 and t_5 being selected to give the appropriate area under the acceleration plot (i.e. velocity). The resulting velocity profile is shown in Figure 6. If it is assumed that the manoeuvre is initiated with the helicopter aligned to the earth x-axis, with its centre of gravity coinciding with the origin of the earth fixed reference frame, and that constant heading and altitude are maintained, the manoeuvre specification becomes

$$x(t) = \int_0^t V(t)\, dt, \quad y(t) = 0,$$
$$z(t) = \text{const.}, \quad \psi(t) = 0 \tag{12}$$

Figures 5 and 6 both show symmetrical profiles, this only occurs if the maximum acceleration and maximum deceleration are equal.

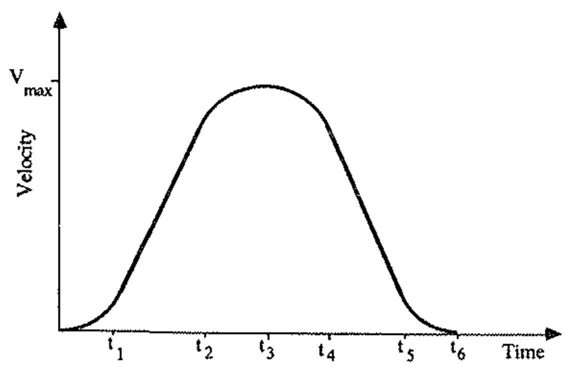

Figure 6 : Velocity Profile for an Acceleration and Deceleration MTE

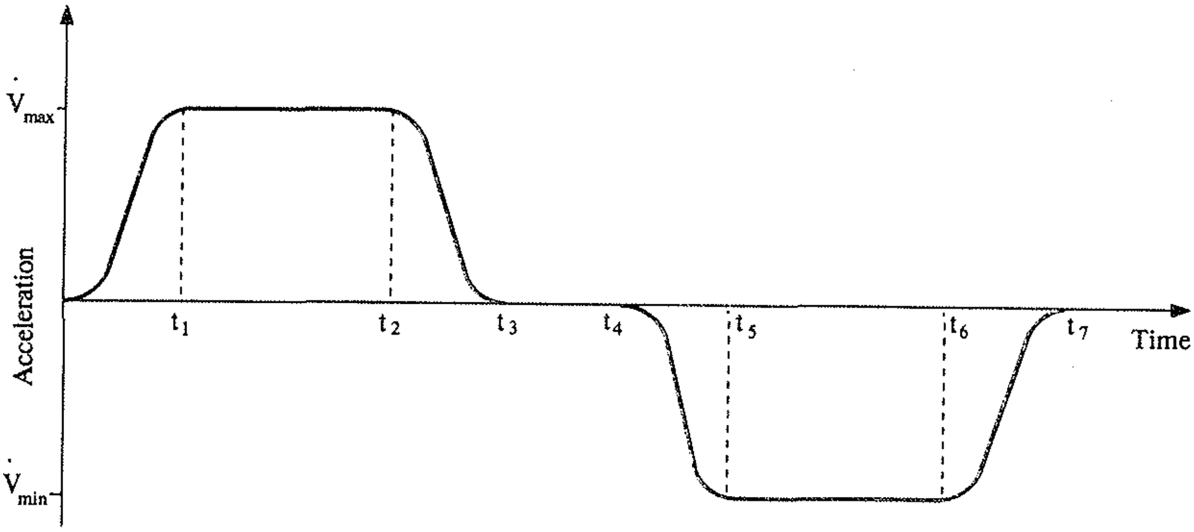

Figure 7 : Acceleration Profile for a Rapid Sidestep MTE

3.3 Rapid Sidestep

The description of this manoeuvre given in Ref. 1 is similar to that of the previous manoeuvre in that accelerations and times are specified. Here an aggressive lateral translation is initiated from the hover until a velocity between 30 and 45 knots is reached. This velocity is to be maintained for approximately 5 seconds after which the helicopter is to be decelerated back to the hover. As in the previous manoeuvre, maximum acceleration and deceleration have to be achieved 1.5 and 3 seconds from their initiation, whilst constant heading and altitude are to be maintained throughout. Considering the similarity of the two descriptions it is perhaps no surprise that they can be modelled in a similar way. Figure 7 shows the proposed acceleration profile, which satisfies the above conditions provided

$$t_1 \le 1.5s, \quad t_4 - t_3 \approx 5s, \quad t_5 - t_4 \le 3s,$$

$$30 \le V(t_3) \le 45 \text{ knots}, \qquad \int_0^{t_7} \dot{V}(t)\,dt = 0 \tag{13}$$

where

$$V(t_3) = \int_0^{t_3} \dot{V}(t)\,dt$$

It is also assumed that

$$t_3 - t_2 = t_1, \qquad t_7 - t_6 = t_5 - t_4 \tag{14}$$

Cubic polynomial functions of time are again used to model the three transient sections, their coefficients being functions of the component times and the maximum acceleration and deceleration. If the same initial conditions as in the acceleration/deceleration MTE are assumed, (the fuselage pointing along the earth x-axis with the c.g. at the origin) then the manoeuvre specification becomes

$$x(t) = 0, \quad y(t) = \int^t\!\!\int^t \dot{V}(t)\,dt\,dt,$$

$$z(t) = \text{const.}, \quad \psi(t) = 0 \tag{15}$$

3.4 Rapid Bob-up and Bob-down

This manoeuvre is also initiated in the hover, from which the helicopter has to bob-up to clear a 7.6m high obstacle, acquire a target, then return to the initial position. The whole manoeuvre is to take less than 8 seconds, whilst the target acquisition time is to be less that 4 seconds. In this case it was found to be more convenient to specify the altitude as a function of time, as shown in Figure 8. This function is suitable provided that the following conditions are satisfied

$$t_3 \le 8s, \qquad t_2 - t_1 \le 4s, \qquad h = 7.6m \tag{16}$$

A mathematical representation of the altitude plot shown in Figure 8 can be obtained by using fifth order polynomial functions of time for the bob-up and bob-down sections:

$$z(t) = at^5 + bt^4 + ct^3 + dt^2 + et + f \tag{17}$$

A fifth order polynomial is used in order to give continuity in acceleration. The bob-up function can be found by considering the boundary conditions

i) $t = 0, \quad z = 0, \quad \dot{z} = 0, \quad \ddot{z} = 0$

ii) $t = t_1, \quad z = -h, \quad \dot{z} = 0, \quad \ddot{z} = 0$

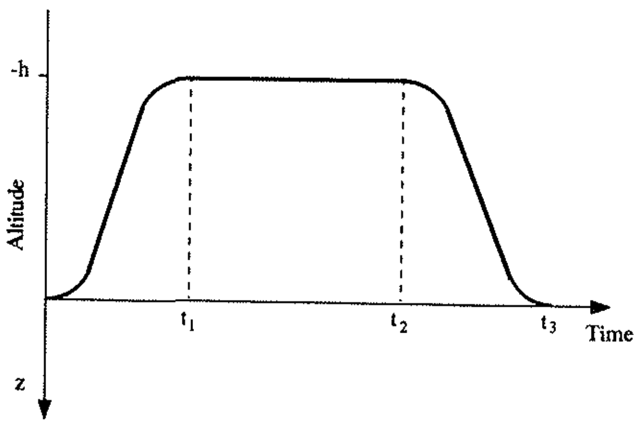

Figure 8 : Altitude Profile for a Bob-up and Bob-down MTE

which gives the altitude function

$$z(t) = \left[-6\left(\frac{t}{t_1}\right)^5 + 15\left(\frac{t}{t_1}\right)^4 - 10\left(\frac{t}{t_1}\right)^3 \right] h \qquad (18)$$

A similar set of boundary conditions are obtained for the bob-down portion, which when applied to the polynomial, (17), allow the corresponding coefficients to be obtained. If the desired target acquisition time is given, and it is assumed that the time to complete the bob-up is the same as the time to complete the bob-down (i.e. t_3-t_2=t_1) then solution for the polynomial coefficients is trivial. As in the previous manoeuvres, it is assumed that the manoeuvre begins at the earth axes origin, and that heading is maintained throughout the manoeuvre, so that the manoeuvre specification is completed by

$$x(t) = y(t) = \psi(t) = 0 \qquad (19)$$

3.5 Pull up/Push over

The description of this manoeuvre in Ref. 1 rests on a definition of the load factor as a function of time. Starting from a level trimmed flight condition with maximum continuous power, a load factor of at least 2g is attained within one second of the start of manoeuvre. It is maintained for at least one second, before a transition to a push over of not greater than 0g. The transition is to take less than two seconds, and the push over sustained to achieve the airspeed at manoeuvre entry. During the manoeuvre it is a requirement that the angular deviations in roll and yaw should not exceed 10 degrees.

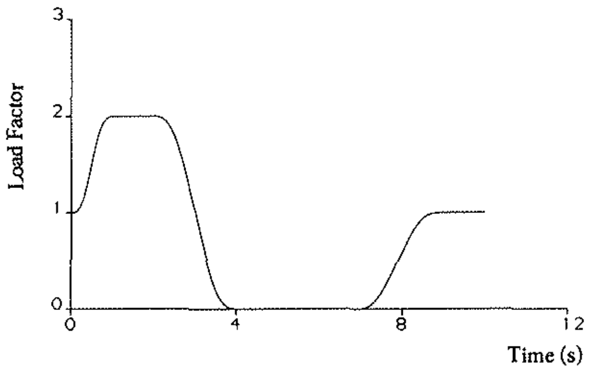

Figure 9 : Load Factor Distribution in Pull-up/Push-over MTE

Figure 9 shows a reasonable interpretation of this description as a load factor profile. Initially the load factor, n, measured in units of g, is unity, between the initial time t=0 and time $t=t_1$, (1 second) a smooth transition to load factor of 2 is made by a polynomial of degree 5 satisfying

$$\text{i)}\ t = 0,\ \ n = 1,\ \ \dot{n} = 0,\ \ \ddot{n} = 0$$
$$\text{ii)}\ t = t_1,\ \ n = 2,\ \ \dot{n} = 0,\ \ \ddot{n} = 0$$

It remains constant at a value of 2 until time $t=t_2$ (2 sec.) where begins a similar smooth transition to a zero load factor achieved at $t=t_3$ (4 sec.) satisfying

$$\text{i)}\ t = t_2,\ \ n = 2,\ \ \dot{n} = 0,\ \ \ddot{n} = 0$$
$$\text{ii)}\ t = t_3,\ \ n = 0,\ \ \dot{n} = 0,\ \ \ddot{n} = 0$$

The zero value is maintained until time $t=t_4$, and a smooth transition is made back to unity load factor at $t=t_5$.

$$\text{i)}\ t = t_4,\ \ n = 0,\ \ \dot{n} = 0,\ \ \ddot{n} = 0$$
$$\text{ii)}\ t = t_5,\ \ n = 1,\ \ \dot{n} = 0,\ \ \ddot{n} = 0$$

The values of t_4 and t_5 remain to be chosen, since they are not explicitly specified in the description of the manoeuvre. The return to unity load factor from its zero value is not intended to be a demanding part of the task, so we have halved its severity compared to other transitions and set its duration at 2 seconds, therefore t_5-t_4=2. The value of t_5 is determined by recalling that the airspeed should have returned to its original value at the end of the manoeuvre, therefore t_5 is adjusted until the value of the airspeed at t_5 is equal to that at the start of the manoeuvre. The load factor in terms of climb angle γ and airspeed, V is

$$n = \frac{V\dot{\gamma}}{g} + \cos\gamma \qquad (20)$$

which when rearranged according to

$$\dot{\gamma} = \frac{g(n - \cos\gamma)}{V} \qquad (21)$$

can be solved for γ once the airspeed V is known throughout the manoeuvre. There is little information about the variation of airspeed, and directly imposing a predetermined profile for it does not seem to be in the spirit of the task. The view taken in the current work is to assume that during the manoeuvre any gain in potential energy is balanced by a loss of translational kinetic energy, so that as the helicopter gains height during the pull up airspeed bleeds away, and correspondingly the loss of height in the latter stages of the push over will recover the lost airspeed. The equation expressing this balance is

$$\dot{V} = -g\sin\gamma \qquad (22)$$

The differential equations (21) and (22) are solved subject to the initial conditions $V(0)=V_{trim}$ (V_{trim} being the trim airspeed at manoeuvre entry) and $\gamma(0)=0$. The equations are solved with particular choice of t_5, and t_5 is adjusted until the exit conditions $V(t_5)=V_{trim}$ is satisfied. Figures 10 and 11 show the profiles of flight path angle and airspeed which result from the load factor of Fig. 9.

From airspeed and climb angle, the flight path coordinates are easily obtained from equations (4) and (6), noting that the track angle, χ, is zero, which are conveniently integrated in the same scheme as (20) and (21), and the manoeuvre definition is completed by setting the heading angle, ψ, to zero for the whole manoeuvre.

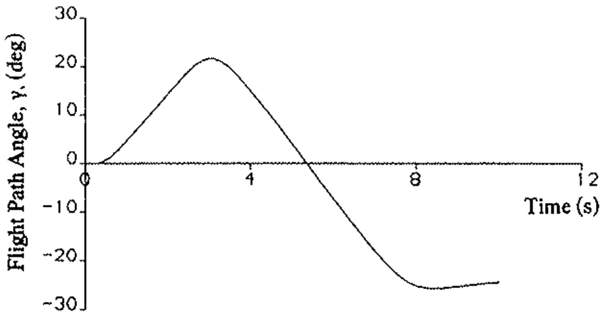

Figure 10 : Flight Path Angle Time History for Pull-up/Push-over MTE

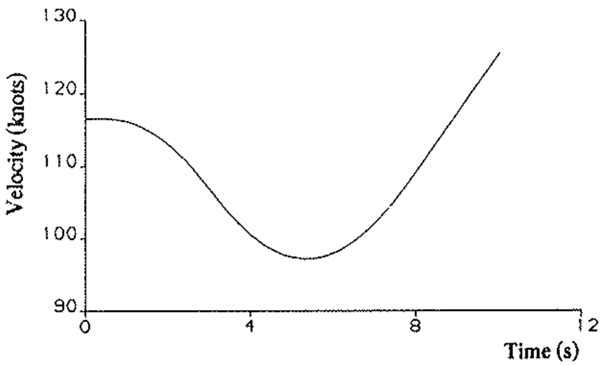

Figure 11 : Velocity Time History for Pull-up/Push-over MTE

3.6 Transient Turn

The object of this manoeuvre is to perform a 180 degrees heading change in less than 10 seconds from an initial velocity of 120 knots, whilst maintaining constant height. The flight path could be considered as simply a semi-circular arc, however as the manoeuvre begins and ends with straight line flight, this would impose discontinuities in the turn rate function, and hence in the accelerations of the helicopter. As well as being unrealistic this is undesirable for inverse simulation where the acceleration time history forms part of the input signal to the mathematical model. To overcome this problem, as discussed at the beginning of this section, the turn rate function is specified as opposed to the flight path co-ordinates. The function used is similar in form to the altitude function in the bob-up/bob-down manoeuvre presented above. As turn rate is given by

$$\dot{\chi}(t) = \frac{V(t)}{R} \qquad (23)$$

where R is the radius of curvature, this shape represents a flight path consisting of a circular path (constant turn rate) with entry and exit transients. The boundary conditions to be satisfied are

$$1)\, t = 0, \quad \dot{\chi} = 0, \quad \ddot{\chi} = 0$$
$$2)\, t = t_1, \quad \dot{\chi} = \dot{\chi}_c, \quad \ddot{\chi} = 0$$
$$3)\, t = t_2, \quad \dot{\chi} = \dot{\chi}_c, \quad \ddot{\chi} = 0$$
$$4)\, t = t_3, \quad \dot{\chi} = 0, \quad \ddot{\chi} = 0$$

which are satisfied by using cubic polynomial functions of time for the transients, as opposed to the fifth order polynomials used in the bob-up/down. The complete turn rate function is given by

$$\dot{\chi}(t) = \left[-2\left(\frac{t}{t_m}\right)^3 + 3\left(\frac{t}{t_m}\right)^2\right]\dot{\chi}_c \qquad 0 < t < t_1$$

$$\dot{\chi}(t) = \dot{\chi}_c \qquad t_1 < t < t_2 \qquad (24)$$

$$\dot{\chi}(t) = \left[2t^3 - 3(t_3 + t_2)t^2 + 6t_3 t_2 t - (3t_3 - t_2)t_2^2\right]\left[\frac{\dot{\chi}_c}{(t_3 - t_2)^3}\right] + \dot{\chi}_c \qquad t_2 < t < t_3$$

If it is assumed that the proportion of the track angle covered in the entry and exit transients is given by a factor, k, then

$$k\pi = \int_0^{t_1} \dot{\chi}(t)\,dt, \qquad (1-2k)\pi = \int_{t_1}^{t_2} \dot{\chi}(t)\,dt, \qquad (25)$$

$$k\pi = \int_{t_2}^{t_3} \dot{\chi}(t)\,dt$$

Combining this information with the turn rate functions (24) is sufficient to allow the component times and the turn rate in the circular section, χ_C to be calculated. The flight path can then be readily found (noting that $\gamma=0$, as height is constant) from equations (4, 5, 6). To complete the manoeuvre specification it is assumed that the turn is performed without sideslip (i.e. $\beta(t)=0$).

4. Using Inverse Simulation at the Conceptual Design Stage

In this section it is proposed to demonstrate the ways in which inverse simulation may be used in the early stages of design to aid investigation of the performance of a planned configuration. The designer's first task is to choose a series of manoeuvres which he feels is most appropriate to the helicopter's role. Although there are any number of possible manoeuvres which might yield useful information, those defined by the authors of Reference 1 are most useful as a guide for this selection particularly as required performance limits are also specified. Having specified the manoeuvre-set, and assuming that the mathematical model is generic in form, inverse simulation can help answer the following questions:

1. Can the helicopter, with known power and control limits, fly the manoeuvres without exceeding any vehicle limits, and within the given performance criteria ?

If the answer to question 1 is NO then it is further possible to answer the question

2. What configurational changes can be made, if any, which will allow the requirements to be met ?

If the answer to question 1 is YES then it is possible to answer the questions

3. How much control margin will the pilot have ?

4. What are the centre of gravity and mass limitations on the helicopter flying each manoeuvre?

The importance of the answer to question 3 lies in the consideration of the manoeuvrability, agility and handling qualities of the helicopter, control margin influencing all three of these characteristics.

The ability of inverse simulation to answer these questions is best illustrated by presenting some results. A set of configurational data representing a hypothetical battlefield utility helicopter has been prepared. The data has been chosen intentionally to give a helicopter with poor performance by setting some of the key parameters to slightly unrealistic values. This is simply to highlight the improvement in performance when these parameters are adjusted. The full configurational data set can be used in the mathematical model to perform inverse simulations of this helicopter flying some or all of the previously described MTEs.

4.1 Improvement of Initial Design

It is assumed that the initial design, Configuration 1, consisted of a helicopter with a mass of 4000kg and a fully articulated, 4 bladed rotor of low solidity. Guidance on the choice of parameter values and control limits was obtained from existing configurational data sets, (Aerospatiale Puma and Westland Lynx), [11]. Table 1 gives some of the most important parameters, and Table 2 gives the control limits. The configurational data set was completed by using parameters from an existing mathematical model of a similar class of helicopter. Using this data set it was possible to run simulations of Configuration 1 flying each of the MTEs described in Section 3, however the results from two manoeuvres only will be presented here : the Acceleration and Deceleration, and the Rapid Slalom.

The manoeuvre parameters are chosen to satisfy the requirements given by the MTE descriptions given in Reference 1. For the Acceleration and Deceleration it was assumed that the maximum velocity reached was 60 knots, and that the maximum and minimum accelerations were 7 and $-7 m/s^2$ respectively. The maximum achieved speed (60 knots) is a minimum requirement, but, as no minimum time or distance is specified, the critical parameter in the manoeuvre definition will be the peak accelerations, and not the maximum velocity. The values for maximum and minimum acceleration were chosen after examination of flight data from similar manoeuvres, [6, 9, 10]. The parameters used for the slalom manoeuvre are as given in Reference 1, a velocity of 60 knots, and a lateral displacement, h, of 15.2m. It is also stipulated in Ref. 1 that the minimum bank angle is to be 50 degrees, and by trial and error it was discovered that this occurs when the manoeuvre time is less than 10 seconds (giving a minimum distance covered in completing the manoeuvre of about 300m).

Figure 12 shows the main rotor collective and longitudinal cyclic controls for the Acceleration and Deceleration MTE flown by Configuration 1. It is apparent from the plot of collective that the rotor of Configuration 1 does not produce sufficient thrust to perform the manoeuvre, and this may also explain why

Parameter	Configuration		
	1 : Articulated Low Solidity	2 : Articulated High Solidity	3: Semi-rigid High Solidity
Aircraft Mass (kg)	4000	4000	4000
Flapping Stiffness (Nm/rad)	50000	50000	150000
Rotor Radius (m)	6.0	6.25	6.25
Blade Chord (m)	0.3	0.35	0.35
No. of Blades	4	4	4
Solidity	0.06366	0.0713	0.0713

Table 1 : Configurational Data

Control	Upper Limit (deg)	Lower Limit (deg)
Collective, θ_0	20.0	-5.0
Long. Cyclic, θ_{1s}	7.0	-14.0
Lat. Cyclic, θ_{1c}	8.0	-8.0
T.R. Coll., θ_{0tr}	30.0	-8.0

Table 2 : Control Limits for all 3 Configurations

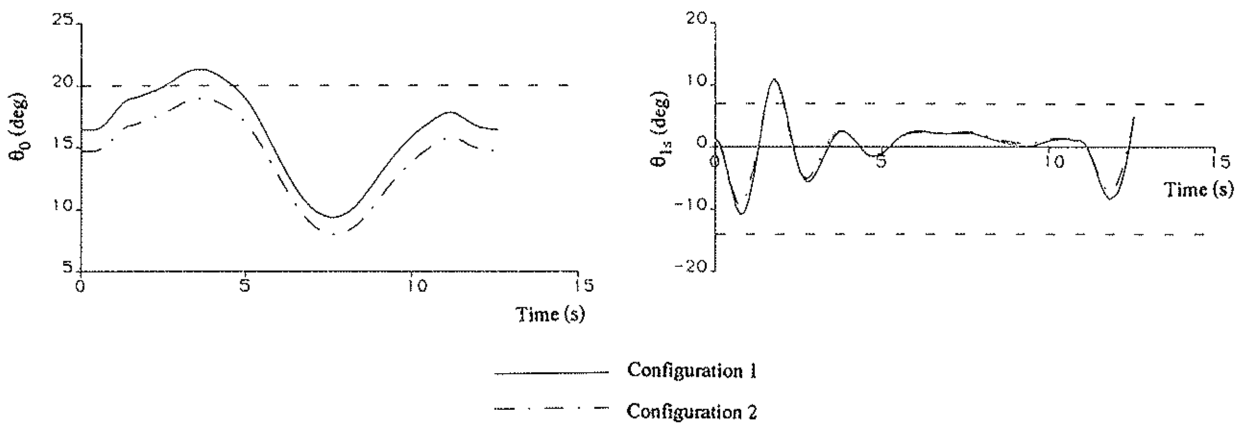

Figure 12 : Control Inputs Required to Fly an Acceleration and Deceleration MTE

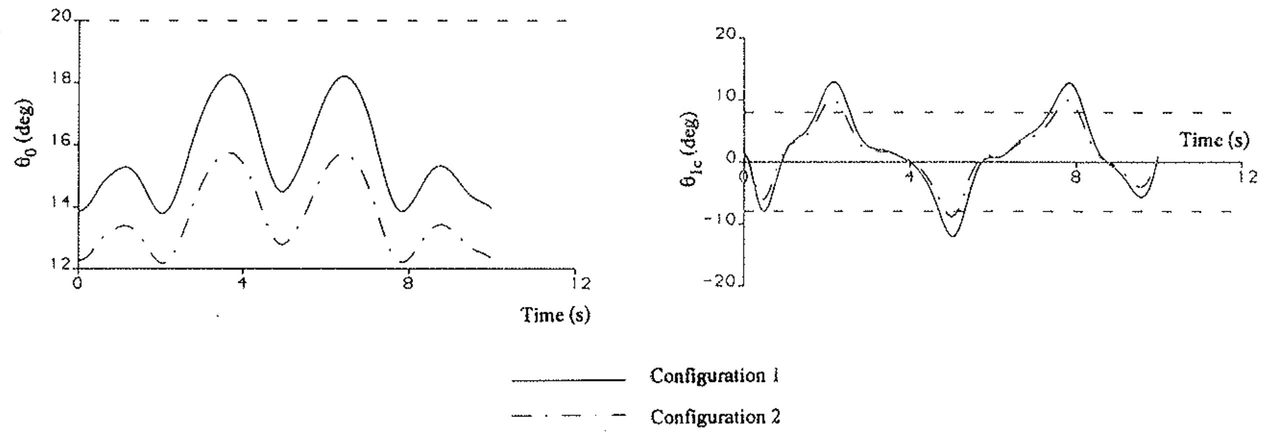

Figure 13 : Control Inputs Required to Fly a Slalom MTE

the longitudinal cyclic limit is exceeded. This result is also observed in Figure 13 which shows the main rotor collective and lateral cyclic control time histories for a Slalom manoeuvre, although in this case the collective limit is approached but not exceeded. Thus it has been demonstrated by use of inverse simulation, that Configuration 1 is incapable of flying these MTEs within the specified limits.

The next question which arises is what parameter changes can be made which will allow the manoeuvres to be flown. As it is obvious that the existing rotor is not producing enough thrust a second configuration (Configuration 2) has been created with the rotor radius increased to 6.25m and the chord to 0.35m. It has been assumed that no significant weight gain was incurred. The resulting control time histories are compared with Configuration 1 in Figures 12 and 13. The effect of this is to reduce the amount of collective required to fly the manoeuvre, in the case of the Acceleration and Deceleration MTE it is now possible for the helicopter to fly the manoeuvre. Maximum power was not exceeded.

Although the increased thrust has helped to reduce cyclic inputs required, in both manoeuvres the cyclic limits (longitudinal in the Accel./Decel. MTE, and lateral in the Slalom) are still exceeded. One way of reducing cyclic inputs would increase the control power available to the pilot by replacing the articulated rotor with a semi-rigid rotor (i.e. one without flapping hinges). To investigate this possibility, a third configuration has been proposed (Configuration 3, Table 1). The flapping behaviour of the rotor is simulated by an equivalent centre spring model, the value of the spring flapping stiffness, K_β being related to the structural stiffness of the blade. A typical value of K_β for an offset hinge, articulated rotor is 50000 Nm/rad, used for Configurations 1 and 2, and this has been increased to 150000 Nm/rad for the semi-rigid rotor helicopter Configuration 3. Again, these values were chosen after consideration of existing helicopters already being modelled by HELISTAB and HELINV. The effect this change has on the cyclic control during the Slalom manoeuvre is shown in Figure 14, where the lateral cyclic displacements have been reduced to below the control limit of 7 degrees. A similar result is achieved for the Acceleration and Deceleration MTE, Figure 15, where there is a large reduction in the peak longitudinal cyclic displacements.

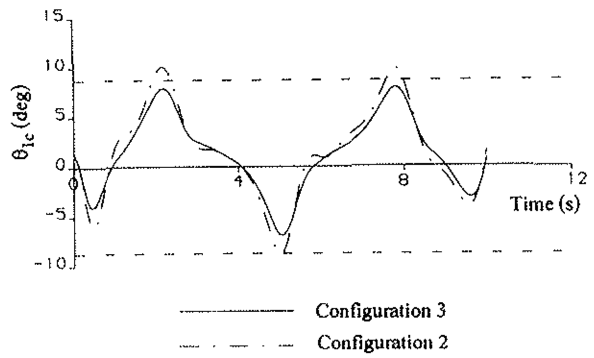

Figure 14 : Lateral Cyclic Input Required to Fly a Slalom MTE

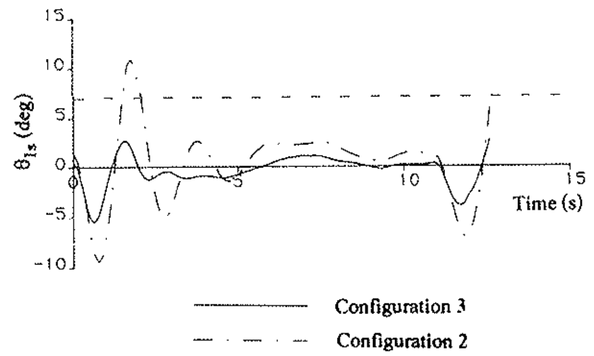

Figure 15 : Longitudinal Cyclic Input Required to Fly an Acceleration and Deceleration MTE

4.2 Measurement of Control Margin

The results above show how inverse simulation may be used to investigate the effects of making parametric changes to the helicopter configuration. Figure 15 shows a clear reduction in the longitudinal cyclic inputs required to fly an Acceleration and Deceleration manoeuvre due to a change in the rotor flapping stiffness. It is evident from this figure that the pilot would have a much greater *Control Margin* flying this manoeuvre with the semi-rigid rotor helicopter. The Control Margin gives a measure of the excess capability that the helicopter has, and consequently can be used as a criteria for measuring performance improvements due to parametric changes, for example. There are perhaps several ways of defining a control margin, here it is assumed to be the difference between the control limit and the control position. More precisely, for a given manoeuvre, having calculated the time history, $\theta_i(t)$, of the helicopter control, θ_i, the Control Margin, C.M. of this control is defined as

$$\text{C.M.} = \frac{1}{t_m}\int_0^{t_m} \mu(\theta_i(t))\, dt \qquad (26)$$

$$\text{where } \mu(\theta_i) = \begin{cases} \theta_{i\max} - \theta_i, & \theta_i > \theta_{ie} \\ \theta_i - \theta_{i\min}, & \theta_i < \theta_{ie} \end{cases}$$

where θ_{imax}, and θ_{imin}, are the upper and lower limits of control θ_i, and θ_{ie}, is the trim value of the control at the entry to the manoeuvre. This is represented graphically in Figure 16, where the above integrals are

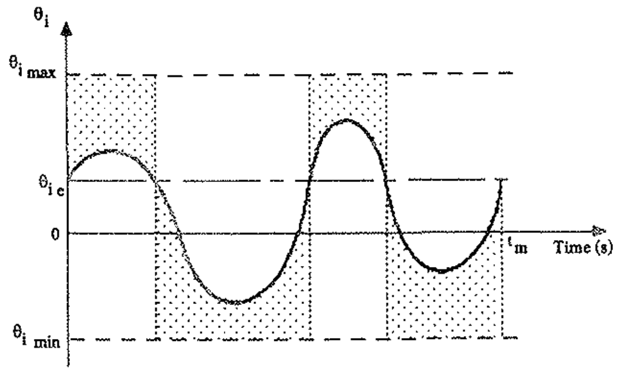

Figure 16 : Function for Determining Control Margin

effectively used to calculate the shaded area. The integral is divided by t_m to average the calculated value. This allows Control Margins from a variety of manoeuvres, possibly with different manoeuvre times, to be compared. A Control Margin can be calculated for each control and each manoeuvre, the results being conveniently presented on a bar chart. Figure 17 shows such a chart for the Control Margins of Configuration 3 flying a series of MTEs. From this chart it is evident that there is a very small collective Control Margin for the Transient Turn MTE. The reason for this is that it is a fairly severe manoeuvre where the 120 knots flight speed and the 10 second manoeuvre time requirements [1] produce bank angles in the region of 70 degrees. If constant height is to be maintained large collective inputs, close to the limiting value, are therefore required.

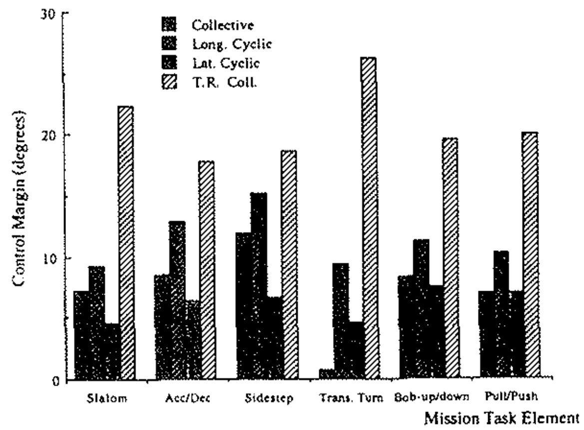

Figure 17 : Control Margins of "Configuration 3" Flying a Series of MTEs

4.3 Centre of Gravity and Mass Limitations

Another use of inverse simulation is in the determination of the c.g. and mass limitations of the helicopter in each manoeuvre. To determine the mass limitation for a specific MTE a series of inverse simulations are performed changing the value of the mass each time until a control limit ,or the maximum power limit, is exceeded. In the case of Configuration 3 flying an Acceleration and Deceleration manoeuvre, increasing the mass to 4450 kg just causes the main rotor collective limit to be exceeded. It was assumed in all of the previous simulation results that the centre of gravity was located directly below the rotor hub. A similar process can be used to determine the limitations on the position of the centre of gravity. Figure 18 shows the envelope of helicopter mass and c.g. limitations for Configuration 3 flying the Acceleration and Deceleration MTE. This envelope was calculated by varying the helicopter mass and c.g. location until the longitudinal cyclic limit was broken. The aft limit is greater than the forward limit because the forward cyclic limit (14 deg.) is greater than the aft cyclic limit (7 deg.), Table 2. Both forward and aft c.g. limits are far in excess of values likely to be encountered in such a small aircraft and it can be concluded the position of the centre of gravity would be unlikely to cause problems in this configuration.

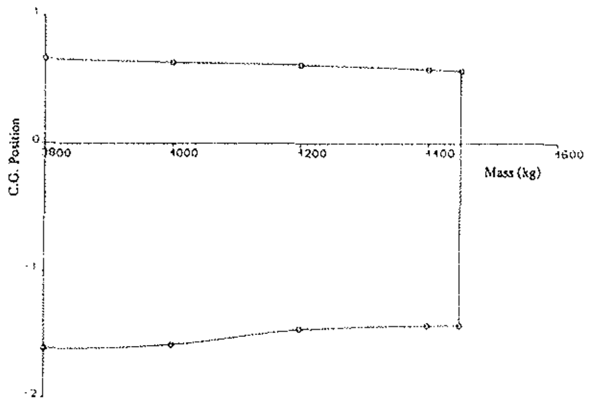

Figure 18 : Centre of Gravity and Mass Envelope for "Configuration 3" Flying Acceleration and Deceleration MTE

5. Conclusions

This paper has described the application of inverse simulation techniques to a subset of the MTE's described in Reference 1. It has shown how inverse simulation has a valuable contribution to make in the development of helicopter designs to satisfy handling qualities requirements based on MTE's. Once a definition of an MTE is available as a defined flight path, then:

(a) The effect of parametric changes on the performance of the helicopter in the execution of the MTEs is directly available.

(b) Information about the available control margins is also available directly from the results of inverse simulation.

As regards the conversion of the MTE descriptions into precise flight path definitions:-

(a) It is possible to create parameterised mathematical descriptions of the MTEs defined in Reference 1. Since the severity of the manoeuvres can be varied by the alteration of a few parameters the sensitivity of a helicopters performance to variations in the MTE severity can be explored.

(b) The mathematical descriptions used in this paper are based on the authors' interpretation of Reference 1. In most cases the detail of the definition does not appear to be critical but there is a need for more flight data from MTE flight trials to provide convincing validation.

It should be clear that there is more work yet to be done to encapsulate the concepts behind the MTE requirements into the flight path definitions necessary for inverse simulation. Even so, sufficient progress has been made to demonstrate the benefits of inverse simulation for design evaluation.

Acknowledgements

The authors wish to thank Dr Gareth Padfield of the Royal Aerospace Establishment, Bedford, for supplying the flight data used in this paper. Work in the field of inverse simulation is currently funded through a Royal Society University Research Fellowship with technical support from the Ministry of Defence.

References

1. Anon, "Handling Qualities Requirements for Military Rotorcraft", Aeronautical Design Standard, ADS-33C, August 1989.

2. Smith, G.A., Meyer, G. "Aircraft Automatic Flight Control System with Model Inversion", Journal of Guidance and Control, Vol. 10, No. 3, 1987.

3. Lane, S.H., Stengel, R.F., "Flight Control Design Using Non-linear Inverse Dynamics", Automatica, Vol. 24, No. 4, 1988.

4. Nannoni, F., Stabellini, A., "Simplified Inverse Simulation for Preliminary Design Purposes", Proceedings of the 15th European Rotorcraft Forum, Amsterdam, The Netherlands, September 1989.

5. Thomson, D.G., Bradley, R., "Development and Verification of an Algorithm for Helicopter Inverse Simulation", Vertica, Vol.14, No. 2, May 1990.

6. Thomson, D.G., Bradley, R., "An Investigation of Pilot Strategy in Helicopter Nap-of-the-Earth Manoeuvres by Comparison of Flight Data and Inverse Simulations", Proceedings of the Royal Aeronautical Society Conference: Helicopter Handling Qualities and Control, London, November 1988.

7. Thomson, D.G., Bradley, R. "An Investigation of Flight Path Constrained Helicopter Manoeuvres by Inverse Simulation", Proceedings of the 13th European Rotorcraft Forum, Arles, France, September 1987.

8. Thomson, D.G., "Evaluation of Helicopter Agility Through Inverse Solution of the Helicopter Equations of Motion", Ph. D. Dissertation, Department of Aeronautics and Fluid Mechanics, University of Glasgow, May 1987.

9. Thomson, D.G., Bradley, R., "Validation of Helicopter Mathematical Models by Comparison of Data from Nap-of-the-Earth Flight Tests and Inverse Simulations", Paper No. 78, Proceedings of the 14th European Rotorcraft Forum, Milan, Italy, September 1988.

10. Thomson, D.G., Bradley, R., Murray-Smith, D.J., "Verification and Validation of Helicopter Flight Mechanics Models", Proceedings of the 3rd European Simulation Congress, Edinburgh, Scotland, September 1989.

11. Padfield, G.D., "A Theoretical Model of Helicopter Flight Mechanics for Application to Piloted Simulation", RAE TR 81048, April 1981.

12. Thomson, D.G., Bradley, R., "Modelling and Classification of Helicopter Combat Manoeuvres", Proceedings of the 17th ICAS Congress, Stockholm, Sweden, September 1990.